infrastructures

MDPI

Article

Carbonation Resistance Performance and Micro-Structure Analysis of Glazed Hollow Bead Insulation Concrete

Xin Huang, Weijing Yao and Jianyong Pang *

School of Civil Engineering and Architecture, Anhui University of Science and Technology, Huainan 232001, China; xinh2017@126.com (X.H.); yaoweijing0713@163.com (W.Y.)

* Correspondence: jypang@aust.edu.cn; Tel.: +86-0554-66685288

Received: 24 August 2019; Accepted: 30 September 2019; Published: 5 October 2019

Abstract: In this paper, the carbonation depths of glazed hollow bead insulation concrete (GHBC) and normal concrete (NC) at different carbonation ages are tested. The microstructure of GHBC and NC before and after carbonation were observed and compared by mercury intrusion porosimetry (MIP), energy dispersive spectrometer (EDS), and X-ray diffraction (XRD). The results showed that NC had better carbonation resistance than GHBC, and GHBC had a carbonation depth of 1.61 times than that of NC at 28 days accelerated carbonation experiment. The microstructural analysis showed that with the decrease of porosity of the samples, the carbon content and $CaCO_3$ content increased after carbonation. The porosity of NC decreased from 14.36% to 13.53%, the carbon content increased from 4.42% to 5.94%, and the $CaCO_3$ content increased from 18.5% to 56.0%. The porosity of GHBC decreased from 22.94% to 20.71%, the carbon content increased from 4.97% to 5.31%, and the $CaCO_3$ content increased from 70.0% to 82.0%. The above results showed that carbon reacts with hydration products $3CaO{\cdot}SiO_2$, $2CaO{\cdot}SiO_2$, and $Ca(OH)_2$ to produce a large amount of $CaCO_3$ which causes a large amount of pores to be filled and refined hence the porosity and pore size were reduced leading to increase in the compactness of the material. From the results obtained, the carbonation depth prediction formula of glazed hollow bead insulation concrete was developed, and carbonation life was predicted.

Keywords: glazed hollow bead insulation concrete; carbonation resistance performance; MIP; EDS; XRD; carbonation depth prediction

1. Introduction

Carbonation refers to the infiltration of carbon dioxide in the air into concrete, which reacts with the alkaline substances in the concrete (C-S-H, ettringite, and unhydrated cement etc.,) to form silicate and water. The carbonation process is not a continuous process. Pre-carbonization produces calcium carbonate, calcium silicate, and other substances to plug the pores and reduce the rate of carbonization. At the later stage of carbonization, concrete causes coagulation shrinkage and crack expansion. Carbonation and decalcification of C-S-H lead to an increase of porosity, and the carbonization process continues. Carbonation leads to a decrease in the pH value of concrete. The passivation film formed on the surface of the steel in a high alkalinity environment is destroyed, which causes the chloride ions adhering to the concrete to be converted into free chloride ions. In severe cases, concrete shrinkage deformation occurs which in-turn affects the structural volume stability [1–5]. Carbonation is an important factor that causes durability problems in concrete structures and reducing service life.

The reduction of the bulk density and the enhancement of thermal insulation has received much attention because of concrete mixing with glazed hollow bead [6,7]. GHBC has remarkable advantages

in heat preservation and fire resistance [8]. In addition, the research also shows that GHBC has an obvious improvement in flexural and shear strength of reinforced concrete [9]. Compared with normal sand, glazed hollow bead lightweight fine aggregate has an obvious difference in shape, density, and surface morphology. Scholars studied their macroscopic physical and mechanical properties [10], thermal insulation performance [11], microstructure [12], and deterioration of mechanical properties after exposure to high temperature [13]. The results showed that the special embedded structure with cement stone was formed by unique micro-pump water storage effect which greatly improves the workability, fluidity, and thermal insulation of the materials, and causes the loss of strength. However, the research of the anti-carbonation properties of the concrete with glazed hollow bead has not been reported.

For rapid carbonation indoor experiments, scholars mostly considered the effects of water-binder ratio, mineral admixtures, aggregate, humidity, temperature, stress state, and other influencing factors on carbonation depth, and finally, a mathematical model was established [14–17]. For example, Luoshu Gong [18], Bogas [19], Ferrer [20], and other scholars have discussed this, focusing on the various influencing factors on the carbonation resistance of materials, factors sorting and weight, and establishment of predictive models. However, the change of microstructure of concrete after carbonation has not been much explored because of the lack of relevant studies on the macroscopic properties of the materials related to the microstructure [21–23]. In this paper, the anti-carbonation law of glazed hollow bead insulation concrete was explored and compared with normal concrete. Mercury intrusion porosimetry (MIP), energy dispersive spectrometer (EDS), and X-ray diffraction (XRD) were used to explore the microstructure changes of the concrete simultaneously. The carbonation resistance mechanism of glazed hollow bead concrete was studied from macroscopic and microscopic perspectives and the carbonation depth prediction model was given.

2. Materials and Methods

2.1. Raw Materials

Cement P·C 42.5 composite Portland cement was adopted whose compressive strengths of 3 d and 28 d were 29.9 MPa and 47.7 MPa, respectively. Moreover, the fly ash was used to increase the workability and later strength of concrete. The chemical composition of cement is shown in Table 1. The use of Grade I fly ash produced by the power plant and its chemical composition content is shown in Table 2. Medium sand was adopted as fine aggregate, and its fineness modulus was 2.8. The glazed hollow bead was used as lightweight fine aggregate and its main performance indicators are shown in Table 3. The coarse aggregate was calcareous gravel with a continuous gradation of 5–15 mm. The admixture was a high-performance water reducing agent.

Table 1. The chemical composition of cement/%.

Material	CaO	SiO_2	Al_2O_3	MgO	SO_3	Fe_2O_3	Ignition Loss
Content	63.11	22.60	5.03	1.46	2.24	4.38	1.18

Table 2. The chemical composition of fly ash/%.

Composition	SiO_2	Al_2O_3	Fe_2O_3	CaO	MgO	Na_2O	Ignition Loss
Content	53.26	34.72	4.07	2.47	0.39	1.90	4.07

Table 3. The performance indicators of glazed hollow bead.

Particle Size/mm	Bulk Density/kg·m^{-3}	Apparent Density/kg·m^{-3}	Cylinder Compressive Strength/MPa	Thermal Conductivity/W·(m·K)$^{-1}$	Refractoriness/°C	Volume Loss Rate of 1 MPa Pressure/%
0.5~1.5	80~120	80~130	≥150	0.032~0.045	1280~1360	38~46

Figure 1 shows the particle size distribution curve of glazed hollow bead.

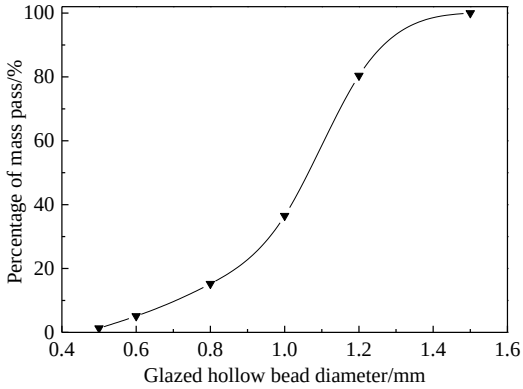

Figure 1. Size distribution curve of glazed hollow bead.

Figure 2 shows the actual photo and microstructure of the experimental glazed hollow bead. It is a non-metallic lightweight thermal insulation material, which was formed by crushing and sieving rosin rock ore then heating it at high temperature to allow instantaneous combustion, expansion, and vitrification of the surface. After the surface was vitrified and closed, it acquired a spherical fine particle size with a honeycomb porous structure inside. This special structure prolonged the heat transfer path inside the material, increased the internal pores, allowed heat to propagate both in the concrete and air (even though air is a good heat insulating material with a thermal conductivity of only 0.026 W/(m·K) [24]) which led to an increase in heat dissipation loss and improving the heat insulation capacity while the outer surface vitrification is spherical. During the concrete mixing process, it was easily subjected to crushing and vibration which resulted in strength loss.

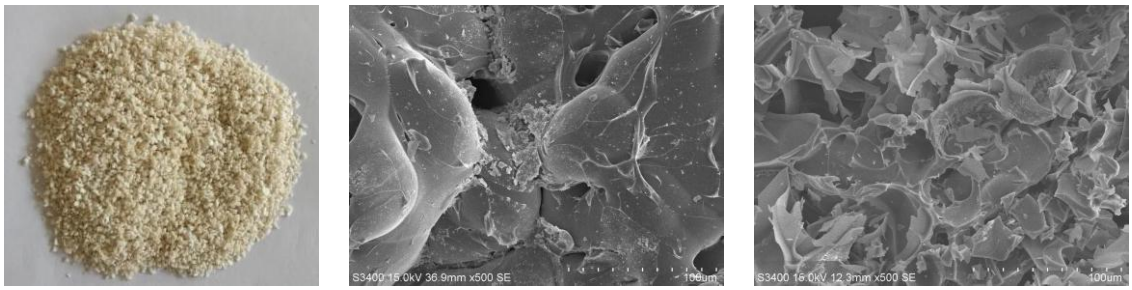

(**a**) (**b**) (**c**)

Figure 2. Actual photo and microstructure morphology of glazed hollow bead: (**a**) Actual photo, (**b**) Core and (**c**) Shell.

2.2. Mixing Ratio Design of Concrete

Before the test, the glazed hollow bead soaked in water for 1 hour, and the water-binder was adjusted by the test to make sure that there was consistency in water consumption. The amount of each raw material is shown in Table 4. The basic performance test results of normal concrete (NC) and glazed hollow bead insulation concrete (GHBC) are shown in Table 5.

It can be seen from Table 5 that the apparent density, compressive strength, and thermal conductivity of the concrete are reduced to different degrees after mixing with the glazed hollow bead lightweight aggregate. The 28-d compressive strength decreases by about 29%, and the thermal conductivity decreases by about 26%. The moisture content is improved because of good water retention of the glazed hollow bead. The soaking treatment of glazed hollow bead greatly improved the workability and fluidity of the mixture, which accords with the building materials development trend of the lightweight, good workability, and thermal insulation.

Table 4. Mix proportions of concrete/kg/m^3.

Number	Cementing Material		Gravel	Fine Aggregate		Water	Water Reducer	Water Cement Ratio
	Cement	Fly Ash		Sand	Glazed Hollow Bead			
NC	421	47	856	856	/	177.84	4.68	1:0.38
GHBC	421	47	856	571	100	168.48	4.68	1:0.36

Table 5. Physical and mechanical properties of concrete.

Number	Workability		Compressive Strength/MPa		28 d Apparent Density/kg·m^{-3}	28 d Moisture Content/%	28 d Thermal Conductivity/W·(m·K)$^{-1}$
	Slump/mm	Slump Flow/mm	3 d	28 d			
NC	175	350	15.61	36.80	2272	1.10	1.65
GHBC	200	410	8.12	26.13	2102	1.73	1.22

2.3. Experimental Method

Soaking of glazed hollow bead was carried out for 1 hour before the preparation of concrete. According to the process shown in Figure 3, and specification for carbonization test in Standard for *Testing Method of Long-term Performance and Durability of Ordinary Concrete* GB/T50082-2009 of the People's Republic of China, concrete test specimens with sizes of 400 mm × 100 mm × 100 mm were made. The specimens were cured for 28 days under curing conditions of relative humidity ≥95% and temperature (20 ± 2) °C. The concrete carbonation box was used and CO_2 concentration (20 ± 3)%, relative humidity (75 ± 5)%, temperature (20 ± 2) °C were set. The depths of carbonation were measured for the carbonation age of 3, 7, 14, and 28 days. The cement stone part specimens of the NC and GHBC before and after carbonation of 28 days were selected for mercury intrusion porosimetry (MIP), energy dispersive spectrometer (EDS), and X-ray diffraction (XRD).

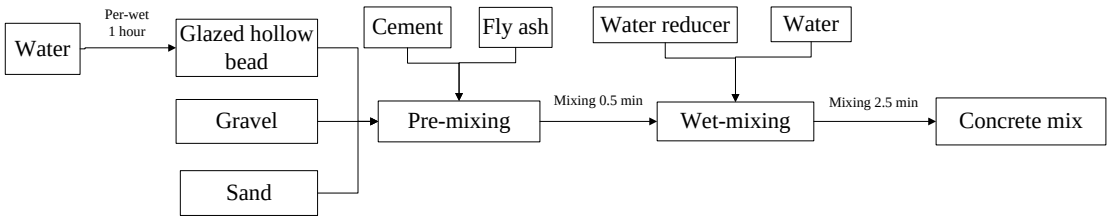

Figure 3. Forming process of concrete.

3. Results and Discussion

3.1. Carbonation Depth Changes with Ages

Cube specimens were split in the middle and sprayed with a 1% phenolphthalein alcohol solution (20% distilled water). After about 30 seconds, the depth of carbonization was measured with a ruler. The test results are shown in Figures 4 and 5. Figure 4 shows the carbonation depth under different carbonation ages of NC and GHBC. The changes of carbonation depth were calculated from the test data in Figure 5. It can be seen from the figures:

(1) The changes regularity of the carbonation depth of NC and GHBC is the same. As the carbonation age increased, the carbonation depth gradually increased while the carbonation rate gradually decreased. The carbonation rate was the fastest within 3 days, followed by 3 to 14 days, and became flat after 14 days. This was because CO_2 reacts with $Ca(OH)_2$ and hydrated calcium

silicate to form $CaCO_3$ in the concrete, which blocks the internal pores of the concrete hence hinders the CO_2 diffusion channel and weakens the carbonation reaction.

(2) After 28 days of carbonation, the carbonation depth of NC and GHBC were 12.25 mm and 19.69 mm, respectively. It can be seen that the depth of GHBC was increased by about 60.73% compared with NC, which indicates that the carbonation resistance of concrete was weakened by mixing glazed hollow bead. This is because the glazed hollow bead lightweight aggregate is loose, porous, and the permeability is high. The compactness of the cement stone is reduced by glazed hollow bead replacing some sand fine aggregates. The CO_2 invades the interior of the concrete and spreads in the pores of the glazed hollow bead which established a bridge between the concrete surface and the interior making the carbonation resistance of GHBC inferior to that of NC. The related research on ceramist lightweight aggregate concrete shows that the carbonation speed of lightweight aggregate concrete is 0.8–1.0 times faster than that of the normal concrete [25,26].

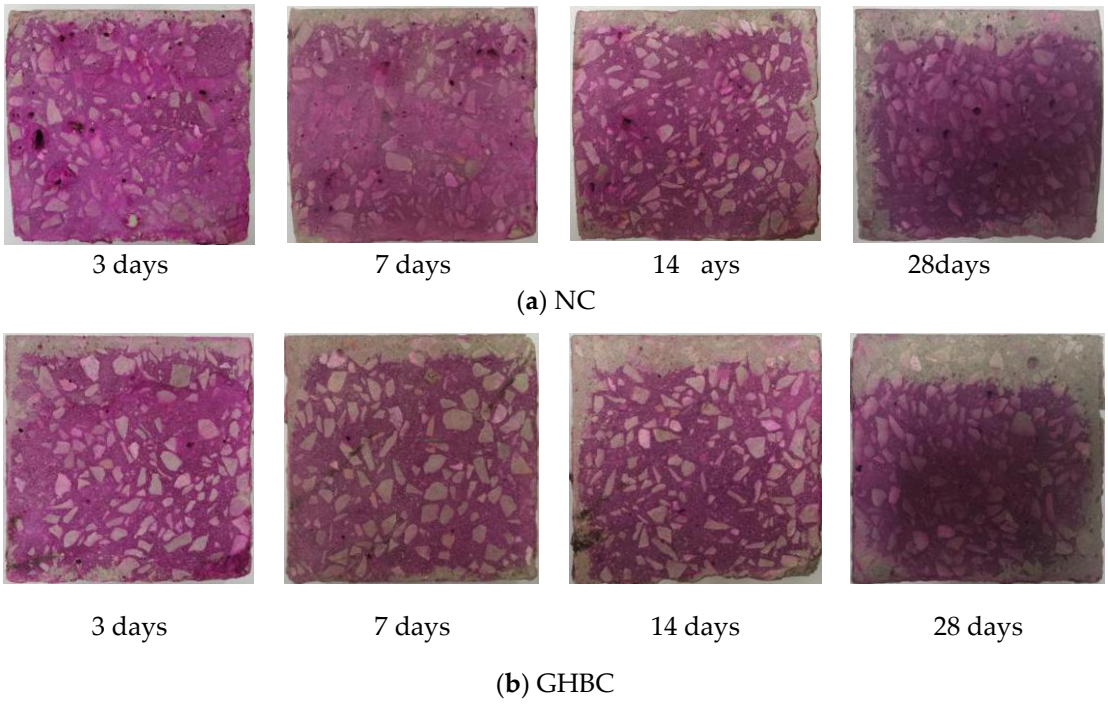

Figure 4. The photo of carbonation depth under different carbon ages of concrete.

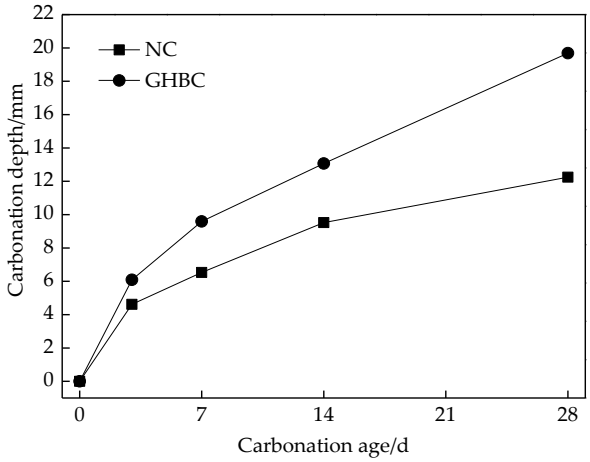

Figure 5. The variation of carbonation depth of concrete with age.

3.2. Microstructure Analysis

As a structural material, the internal microstructure of concrete is closely related to its carbonation resistance. Therefore, the mercury intrusion porosimetry (MIP), energy dispersive spectrometer (EDS), and X-ray diffraction (XRD) were used to study the pore structure and material composition of concrete in order to discuss the mechanism of carbonation resistance of NC and GHBC.

3.2.1. MIP Analysis

Mercury intrusion porosimetry (MIP) was used to quantitative analyze the porosity, pore size distribution, and compactness of concrete specimens before and after the carbonation experiment of 28 days. The results are shown in Table 6. The pore size distribution is shown in Figure 6, and the pore area distribution is shown in Figure 7.

Table 6. The pore characteristic parameters of samples.

Number	Before Carbonation Test			After Carbonation Test		
	Total Pore Area/mL·g^{-1}	Average Pore Diameter/mm	Porosity/%	Total Pore Area/mL·g^{-1}	Average Pore Diameter/mm	Porosity/%
NC	17.80	15.10	14.36	10.83	13.10	13.53
GHBC	20.71	30.70	22.94	10.58	18.30	20.71

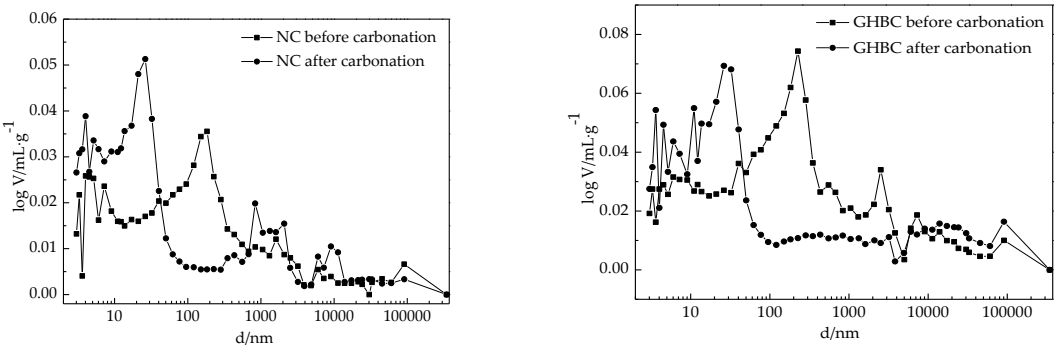

(**a**) (**b**)

Figure 6. The pore size distribution of samples: (**a**) NC and (**b**) GHBC

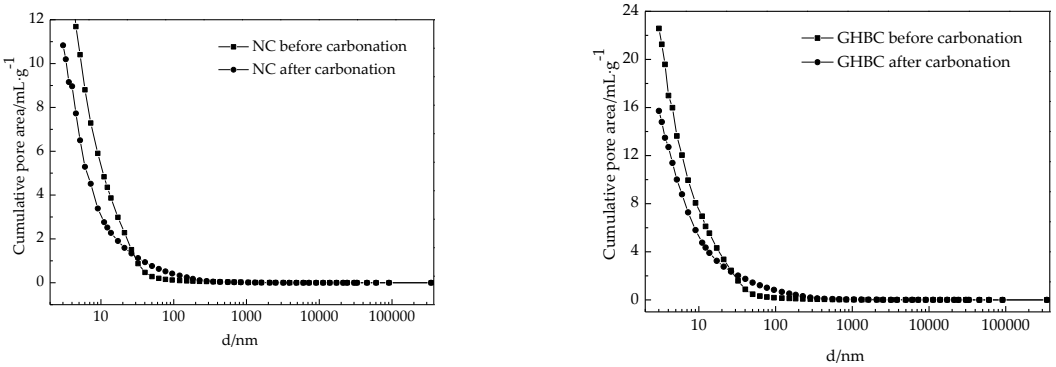

(**a**) (**b**)

Figure 7. The pore area distribution of samples: (**a**) NC and (**b**) GHBC

It can be seen from Table 6 that the total pore area, average pore diameter, and the porosity of the concrete were certainly improved with the addition of glazed hollow bead into the concrete. The total pore area increased from 17.80 mL/g to 20.71 mL/g, the average pore diameter increased from

15.10 nm to 30.70 nm, and the porosity increased from 14.36% to 22.94%. This indicates that loose and porous characteristics of glazed hollow bead lead to the growth of cement stone pores and the internal curing effects of water storage also provided convenience for CO_2 intrusion. After the carbonation experiment, the porosity of the concrete certainly decreased. The total pore area, average pore diameter, and porosity of NC decreased to 10.83 mL/g, 13.10 nm and 13.53%, respectively. And the total pore area, average pore diameter, and the porosity of GHBC decreased to 10.58 mL/g, 18.30 nm, and 20.71%. This indicates that a large number of pores were filled, and refined after carbonation, that is to say, the pore size is reduced and the porosity is decreased.

Figure 6 shows the quantitative analysis of the pore size distribution of the samples. It showed that after the carbonation experiment, the area of the pores larger than 30 nm was greatly reduced, the area of the pores smaller than 10 nm was increased, and the larger the pore size the smaller the logarithm of mercury volume. Figure 7 shows the quantitative analysis of the pore area distribution of the samples. It showed that after the carbonation experiment, the cumulative pore area distribution of each pores were decreased corresponding to the pore size distribution and the larger the pore size, the smaller the cumulative pore area. This is because the CO_2 intrusion into the concrete reacted with the cement hydrates $Ca(OH)_2$, $3CaO{\cdot}SiO_2$, and $2CaO{\cdot}SiO_2$ as per the chemical reactions equation (1) to (4), resulting in a large amount of $CaCO_3$ precipitation. As a result, a large number of pores are filled and refined hence the porosity is decreased. Meanwhile, as the CO_2 intrusion rate and carbonation rate was lowered, the density and strength of the concrete increased macroscopically [27,28].

$$CO_2 + H_2O \rightarrow H_2CO_3 \quad (1)$$

$$Ca(OH)_2 + H_2CO_3 \rightarrow CaCO_3 \quad (2)$$

$$3CaO{\cdot}2SiO_2{\cdot}3H_2O + 2H_2CO_3 \rightarrow 3CaCO_3 + 2SiO_2 + 6H_2O \quad (3)$$

$$2CaO{\cdot}SiO_2{\cdot}4H_2O + 2H_2CO_3 \rightarrow 2CaCO_3 + SiO_2 + 6H_2O \quad (4)$$

3.2.2. EDS Analysis

Energy dispersive spectrometer (EDS) was used to analyze the elements of a plurality specific points or areas of specimens before and after carbonation experiment of 28 days. For each sample, two points and areas with significant features were selected for quantitative analysis of the elements then the average weight of each element was quantitatively tested for four regions and the changes of the elements before and after carbonation were compared.

Figures 8 and 9 show the EDS fixed-point test before and after the carbonation of NC and GHBC. It can be seen from the figure that the morphology of cement hydrates is similar before and after the carbonation, and a dense cement stone structure is formed after curing. The selected region elements were quantitatively analyzed, the test results are shown in Table 7. It can be seen that the carbon content of the samples increased after the carbonation experiment. The NC increased from 4.42% to 5.94%, and the GHBC increased from 4.97% to 5.31%, which explained the carbon content of the concrete caused by carbon intrusion after carbonation. The $CaCO_3$ precipitate increases, resulting in a decrease in porosity and pore size.

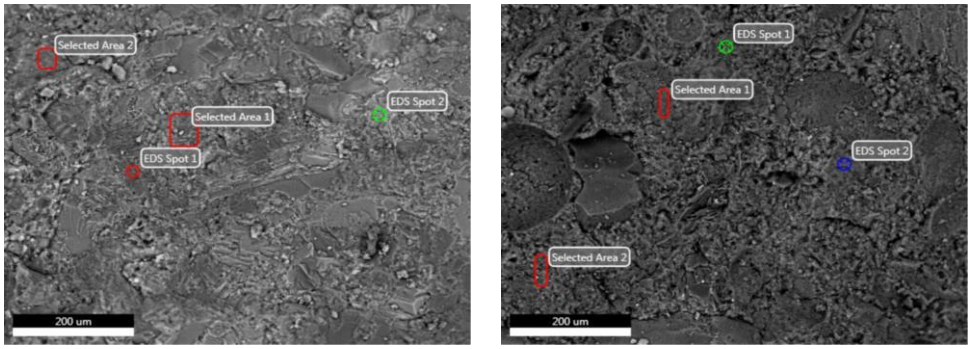

(**a**) Before carbonation test (**b**) After carbonation test

Figure 8. Energy dispersive spectrometer (EDS) test of normal concrete (NC).

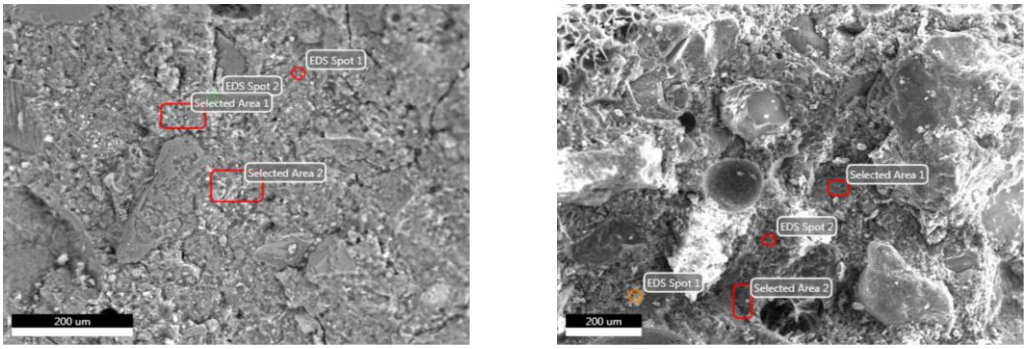

(**a**) Before carbonation test (**b**) After carbonation test

Figure 9. EDS test of glazed hollow bead insulation concrete (GHBC).

Table 7. Fixed-point test results of EDS.

Sample	Element Weight Ratio/%						
	C	O	Al	Si	S	Ca	Fe
Before carbonation test of NC	4.42	53.03	6.41	16.73	0.59	17.04	1.80
After carbonation test of NC	5.94	50.06	7.31	19.36	0.65	13.89	2.78
Before carbonation test of GHBC	4.97	47.65	5.89	11.17	1.00	27.56	1.77
After carbonation test of GHBC	5.31	47.73	4.63	11.48	2.38	26.75	1.75

3.2.3. XRD Analysis

X-ray diffraction was used to test the composition and content of the samples before and after the carbonation experiment of 28 days. The diffraction pattern is shown in Figure 10. The composition and content are shown in Table 8.

As can be seen from Figure 10, the concrete sample is mainly composed of $3CaO{\cdot}SiO_2$, $2CaO{\cdot}SiO_2$, $CaCO_3$, $Ca(OH)_2$, and C-S-H. As can be seen from Table 8, the carbon element invades the insides of the test specimens and a chemical reaction occurs as per the above equation (1) to (4). The $3CaO{\cdot}SiO_2$, $2CaO{\cdot}SiO_2$, and $Ca(OH)_2$ are largely consumed and a large amount of $CaCO_3$ is generated. The test results showed that the $CaCO_3$ content of the NC sample increased from 18.5% before carbonation to 56.0% after carbonation, while the GHBC samples increased from 70.0% to 82.0%.

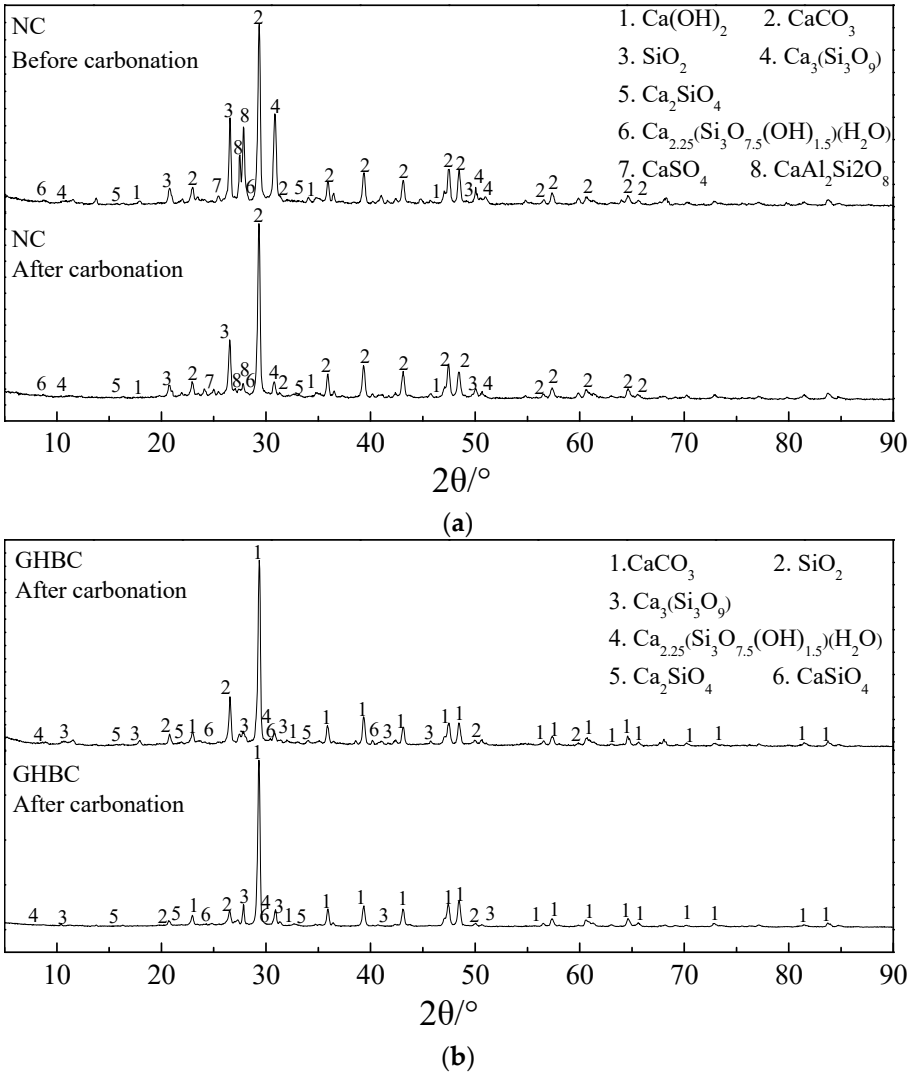

Figure 10. X-ray diffraction (XRD) test of samples: (**a**) NC sample and (**b**) GHBC sample

Table 8. XRD test results of samples.

Sample	Chemical Components Weight Ratio/%							
	$CaCO_3$	$Ca(OH)_2$	$3CaO{\cdot}SiO_2$	$2CaO{\cdot}SiO_2$	C-S-H	SiO_2	$CaSO_4$	$CaAl_2Si_2O_8$
Before carbonation test of NC	18.50	0.40	55.50	0.25	0.13	8.90	0.56	15.9
After carbonation test of NC	56.00	1.55	3.70	0.70	0.24	19.00	3.90	15.40
Before carbonation test of GHBC	70.00	/	4.90	0.60	0.40	20.40	4.11	/
After carbonation test of GHBC	82.00	/	3.10	0.06	2.30	11.80	1.10	/

3.3. Establishment of Carbonation Model

At present, the formula for the development trend of concrete carbonation recommended in the related literature is $X = k\sqrt{t}$, where k is carbonation coefficient, X is carbonation depth, t is carbonation age. The formula assumes that the concrete is an isotropic continuous medium, and the steady diffusion theory is used to simulate the CO_2 diffusion process in concrete which has been widely recognized by researchers [29].

The fitting analysis of the measured carbonation depth data is shown in Figure 11, and the fitting results are shown in Table 9. It can be seen from the table that the correlation coefficients R^2 are both 0.99 for NC and GHBC and the fitting effect was good. It can be seen from the fitting formula that the carbonation resistance of NC is better than that of GHBC. After 28 days of carbonation test, the carbonation depth of GHBC is 1.61 times than that of NC. It indicated that the porous and loose glazed hollow bead form a bridge channel for carbon intrusion, resulting in the weakening of carbonation resistance.

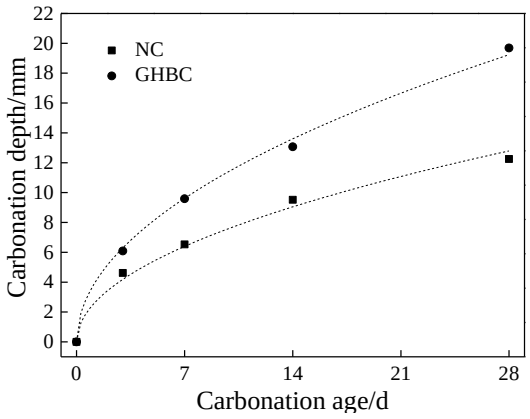

Figure 11. Fitting relationship between carbonation depth and age of concrete.

Table 9. Fitting results of carbonation depth and age of concrete.

Number	Fitting Formula	R^2
NC	$X = 2.42\sqrt{t}$	0.99
GHBC	$X = 3.63\sqrt{t}$	0.99

Note: X represents carbonation depth, mm; t represents carbonation age, d.

3.4. Prediction Carbonation Life of Glazed Hollow Bead Concrete

The effect of concrete carbonation on structural durability is mainly explained by steel corrosion. Therefore, the concrete carbonation allowable index is marked by the fact that steel bars do not rust in concrete. For this reason, the limit state equation of carbonation loss of concrete can be expressed as $Z = C - X_c$, where Z is the thickness of the remaining protective layer of the concrete, mm; C is the carbonation qualification standard for concrete, mm; X_c is the carbonation depth of the concrete, mm.

A large number of experimental data in [30] indicate that there is a relationship between artificial rapid carbonation and natural carbonation.

$$X = X_0 \sqrt{\frac{ct}{c_0 t_0}} \tag{5}$$

where X is the concrete carbonation depth of the age t year, mm; X_0 is the carbonation depth measured by the rapid carbonation test, mm; c is the CO_2 concentration of the air during natural carbonation, generally taking 0.03%; c_0 is the concentration of CO_2 in the environment during rapid carbonation, %; t is the natural carbonation age, d; t_0 is the rapid carbonation age, d.

Predicting the carbonation depth in the natural state according to equation (5). The measured maximum carbonation depth of GHBC is 19.69 mm, that is, X_0 = 19.69 mm, assuming concrete thickness of 25 mm, that is, X = 25 mm, the calculation can be obtained t = 103.06 years. For the carbonization test of vitrified micro-bead concrete, there are few references in the literature. Referring to similar carbonization model literature, the carbonization model is established from some aspects. Song et al. [17] think that water-cement ratio has a great influence on the carbonization resistance of concrete.

At the same age, the carbonization depth of specimens with water-cement ratio of 0.35 is 12 mm, and the water-cement ratio is 12 mm. The carbonization depth of 0.45 is 14 mm. Zhang et al. [31] and others carried out carbonation tests on slag concrete, and put forward a similar prediction model of carbonation life. Tu et al. [32] established a concrete carbonation depth model under stress condition based on the test results.

4. Conclusions

The anti-carbonation characteristics of normal concrete (NC) and glazed hollow bead insulation concrete (GHBC) were studied. Mercury intrusion porosimetry (MIP), energy dispersive spectrometer (EDS), and X-ray diffraction (XRD) were used to investigate the microstructure change of concrete before and after the carbonation test. The following conclusions can be drawn:

(1) The concrete mixed with proper amount of glazed hollow bead can effectively improve the heat insulation capacity and workability while certainly reducing the apparent density and compressive strength. The 28 days compressive strength decreased by about 29%, and the thermal conductivity decreased by about 26%.

(2) Because of the loose porosity of the glazed hollow bead, the compactness of the cement stone is reduced hence facilitates the intrusion of CO_2. After 28 days of carbonation test, the carbonation depth of GHBC and NC were 19.69 mm and 12.25 mm that is the GHBC carbonation depth was 1.61 times than that of NC.

(3) The microstructural analysis showed that the porosity of concrete was reduced and the carbon content increased significantly after carbonation. For NC, the porosity decreased from 14.36% to 13.53%, the carbon content increased from 4.42% to 5.94%, the $CaCO_3$ content increased from 18.5% to 56.0%; for GHBC, the porosity decreased from 22.94% to 20.71%, the carbon content increased from 4.97% to 5.31%, the $CaCO_3$ content increased from 70.0% to 82.0%. It showed that carbon intrusion produces a large amount of $CaCO_3$ precipitation, resulting filing and refining large amount of pores causing porosity and pore size reduction hence compactness of cement stone is increased.

(4) The prediction formula of GHBC was established from experimental data and the fitting effects was good. The carbonation life was also predicted.

Author Contributions: X.H. and W.Y. performed the experiments and analyzed the test data; X.H. and W.Y. wrote the manuscript; J.P. conceived the experiment and provided the guidance and suggestion.

Funding: This research was funded by Doctor Fund Project of Anhui University of Science and Technology, grant number 13190022.

Acknowledgments: The authors acknowledge School of Civil Engineering and Architecture, Anhui University of Science and Technology for their support to perform this research.

Conflicts of Interest: The authors declare no conflict of interest.

References

1. Katpady, D.N.; Hazehara, H.; Soeda, M.; Kubota, T.; Murakami, S. Durability Assessment of Blended Concrete by Air Permeability. *Int. J. Concr. Struct. Mater.* **2018**, *12*, 30. [CrossRef]
2. Ashraf, W. Carbonation of cement-based materials: Challenges and opportunities. *Constr. Build. Mater.* **2016**, *120*, 558–570. [CrossRef]
3. Wu, T. Review on durability of lightweight aggregate concrete in atmospheric environment. *J. Archit. Civil Eng.* **2017**, *34*, 154–162. (In Chinese)
4. Jin, W.L.; Zhao, Y.X. State-of-the-art on durability of concrete structures. *J. Zhejiang Univ. Eng. Sci.* **2002**, *36*, 371–380. (In Chinese)
5. Savija, B.; Lukovic, M. Carbonation of cement paste: Understanding, challenges, and Opportunities. *Constr. Build. Mater.* **2016**, *117*, 285–301. [CrossRef]

6. Tandiroglu, A. Temperature-Dependent Thermal Conductivity of High Strength Lightweight Raw Perlite Aggregate Concrete. *Int. J. Thermophys.* **2010**, *31*, 1195–1211. [CrossRef]
7. Zhang, Z.P. Material and Structural Basic Performance Tests and Theoretical Analysis Research on Glazed Hollow Bead Insulation Concrete. Ph.D. Thesis, Taiyuan University of Technology, Taiyuan, China, 2009. (In Chinese).
8. Zhang, Y.; Ma, G.; Wang, Z.; Niu, Z.; Liu, Y.; Li, Z. Shear behavior of reinforced glazed hollow bead insulation concrete beams. *Constr. Build. Mater.* **2018**, *174*, 81–95. [CrossRef]
9. Zhang, Y.; Ma, G.; Liu, Y.; Li, Z. Flexural performance of glazed hollow bead reinforced concrete beams. *J. Reinf. Plast. Compos.* **2015**, *34*, 1698–1712. [CrossRef]
10. Xiong, H.; Xu, J.; Liu, Y.; Wang, S. Experimental study on hygrothermal deformation of external thermal insulation cladding systems with glazed hollow bead. *Adv. Mater. Sci. Eng.* **2016**, *2016*, 3025213. [CrossRef]
11. Zhao, L.; Wang, W.; Li, Z.; Chen, Y.F. An experimental study to evaluate the effects of adding glazed hollow beads on the mechanical properties and thermal conductivity of concrete. *Mater. Res. Innov.* **2015**, *19*, S5-929–S5-935. [CrossRef]
12. Ma, G.; Zhang, Y.; Li, Z. Influencing Factors on the Interface Microhardness of Lightweight Aggregate Concrete Consisting of Glazed Hollow Bead. *Adv. Mater. Sci. Eng.* **2015**, *2015*, 1–15. [CrossRef]
13. Chai, L.J.; Li, Z.; Liu, Y.Z.; Wang, W. Effect of cooling mode and temperature on micro-structure of glazed hollow bead thermal insulation concrete. *J. Taiyuan Univ. Technol.* **2015**, *46*, 419–423. (In Chinese)
14. Pan, H.K.; Yang, Z.S.; Xu, F.W. Study on concrete structure's durability considering the interaction of multi-factors. *Constr. Build. Mater.* **2016**, *118*, 256–261. [CrossRef]
15. Cho, H.-C.; Ju, H.; Oh, J.-Y.; Lee, K.J.; Hahm, K.W.; Kim, K.S. Estimation of Concrete Carbonation Depth Considering Multiple Influencing Factors on the Deterioration of Durability for Reinforced Concrete Structures. *Adv. Mater. Sci. Eng.* **2016**, *2016*, 1–18. [CrossRef]
16. Song, H.; Niu, D.T.; Li, C.H. Carbonation test of concrete containing mineral admixtures. *J. Chin. Ceram. Soc.* **2009**, *37*, 2066–2070. (In Chinese)
17. Yang, L.D.; Pan, H.K.; Zhu, Y.Z.; Wu, Z.Z. Experimental study of concrete's carbonation resistance under combined action of factors. *J. Build. Mater.* **2008**, *11*, 345–348. (In Chinese)
18. Gong, L.S. Provisions on durability indexes of lightweight aggregate concrete against carbonization. *Concrete* **1991**, *2*, 3–8. (In Chinese)
19. Bogas, J.A.; Real, S.; Ferrer, B. Biphasic carbonation behavior of structural lightweight aggregate concrete produced with different types of binder. *Cem. Concr. Compos.* **2016**, *71*, 110–121. [CrossRef]
20. Ferrer, B.; Bogas, J.A.; Real, S. Service life of structural lightweight aggregate concrete under carbonation-induced corrosion. *Constr. Build. Mater.* **2016**, *120*, 161–171. [CrossRef]
21. Pereira, D.S.D.T.; Da Silva, F.J.; Porto, A.B.R.; Candido, V.S.; Da Silva, A.C.R.; Filho, F.D.C.G.; Monteiro, S.N. Comparative analysis between properties and microstructures of geopolymeric concrete and portland concrete. *J. Mater. Res. Technol.* **2018**, *7*, 606–611. [CrossRef]
22. Xiao, J.; Li, W.; Sun, Z.; Lange, D.A.; Shah, S.P. Properties of interfacial transition zones in recycled aggregate concrete tested by nanoindentation. *Cem. Concr. Compos.* **2013**, *37*, 276–292. [CrossRef]
23. Aguilar, R.A.; Díaz, O.B.; García, J.E. Lightweight concretes of activated metakolin-fly ash binders, with blast furnace slag aggregates. *Constr. Build. Mater.* **2010**, *24*, 1166–1175. [CrossRef]
24. Zhou, S.E.; Lu, Z.Y.; Yan, Y. Study on thermal conductivity model of foamed concrete. *Mater. Rev. Res. Paper* **2009**, *23*, 69–73. (In Chinese)
25. Hu, S.G.; Wang, F.Z. *Lightweight Aggregate Concrete*; Chemical Industry Press: Beijing, China, 2006. (In Chinese)
26. Lo, T.; Tang, W.; Nadeem, A. Comparison of carbonation of lightweight concrete with normal weight concrete at similar strength levels. *Constr. Build. Mater.* **2008**, *22*, 1648–1655. [CrossRef]
27. Song, H.-W.; Kwon, S.-J. Permeability characteristics of carbonated concrete considering capillary pore structure. *Cem. Concr. Res.* **2007**, *37*, 909–915. [CrossRef]
28. Hyvert, N.; Sellier, A.; Duprat, F.; Rougeau, P.; Francisco, P. Dependency of C–S–H carbonation rate on CO_2 pressure to explain transition from accelerated tests to natural carbonation. *Cem. Concr. Res.* **2010**, *40*, 1582–1589. [CrossRef]
29. Niu, D.T. *Durability and Life Forecast of Reinforced Concrete Structure*; Science Press: Beijing, China, 2003. (In Chinese)

30. Zhang, H.Y. The Experimentation Study of Concrete Carbonation Depth and Mathematics Model Founded. Master's Thesis, Northwest Agriculture and Forestry University, Yangling, China, 2006. (In Chinese).
31. Zhang, X.; Zhou, X.; Zhou, H.; Gao, K.; Wang, Z. Studies on forecasting of carbonation depth of slag high performance concrete considering gas permeability. *Appl. Clay Sci.* **2013**, *79*, 36–40. [CrossRef]
32. Tu, Y.; Lu, Z. Experiment and research of presteressed concrete structure in carbonation corrosive environments. *J. Southeast Univ. Nat. Sci. Ed.* **2003**, *33*, 573–576. (In Chinese)